

Relaxation Spectroscopy of the Dielectric β -Relaxation in Poly(*n*-alkyl methacrylate)s by Absorption-Current Measurements. I. Dielectric Relaxation Spectra for Atactic Polymers

Takashi TETSUTANI, Maeko KAKIZAKI, and Teruo HIDESHIMA*

*Department of Applied Physics, Faculty of Engineering,
Hokkaido University, Sapporo 060, Japan.*

(Received November 14, 1981)

ABSTRACT: In order to determine the dielectric relaxation spectra for the β -processes in atactic poly(methyl methacrylate) (PMMA), poly(ethyl methacrylate) (PEMA), poly(*n*-propyl methacrylate) (PnPMA), and poly(*n*-butyl methacrylate) (PnBMA) which were sufficiently separated from the α -processes, absorption current was measured for 10 to 600 s after application of a step voltage at temperatures well below the glass transition temperatures. By applying the Hamon approximation, the data on time dependence of the absorption current were converted to those on the frequency dependence of loss permittivity, and the latter were reduced to master curves by the method of reduced variables. Shift factors gave an activation energy of *ca.* 19 kcal mol⁻¹ irrespective of the side-chain length. Shapes of the β -relaxation spectra for these polymers were the same, but the relaxation strengths for PMMA, PEMA, PnPMA, and PnBMA were in the ratios 1 : 0.8 : 0.6 : 0.5, which correspond to the ratios of their dipolar densities. The β -relaxation spectrum began to sharpen with the increase in temperature above a critical temperature, which was estimated for PMMA and PEMA to be *ca.* 10 and 18°C respectively. A two-site model analysis suggests that the scale of the molecular process for the β -relaxation is as large as a 180°-rotation of the side group about the C-C bond connecting it to the main chain.

KEY WORDS Relaxation Spectroscopy / Dielectric β -Relaxation / Poly(methyl methacrylate) / Poly(ethyl methacrylate) / Poly(*n*-propylmethacrylate) / Poly(*n*-butyl methacrylate) / Absorption Current / Dielectric Relaxation Spectrum / Side-Chain Motion / Glassy State /

It is widely accepted that the β -relaxation in poly(*n*-alkyl methacrylate), which can be observed by both dielectric and mechanical measurements, arises from the rotational motion of the side chain about the C-C bond which links it to the main chain.¹ Many investigations have been made to clarify the effects of such factors as change in molecular structure,²⁻¹⁵ addition of plasticizers,^{16,17} and application of high pressure^{18,19} on the characteristic features of this relaxation. On the basis of the results from these investigations this relaxational motion of the side chain is believed to be governed predominantly by the intrachain interaction, in contrast to the micro-Brownian motion of the main chain for the α -relaxation.

However, there are still only a few data for the relaxation and retardation spectra of the β -process, despite the fact that these are the most important characteristics of the relaxation process. In particular, no dielectric relaxation spectrum for the β -process has as yet been determined under the condition of complete separation from the α -relaxation. Here the term dielectric relaxation is used instead of dielectric retardation, because the former is used conventionally in current papers. In previous papers¹⁰⁻¹² one of the present authors determined the mechanical β -retardation spectra for the four members of poly(*n*-alkyl methacrylate)s using the master curves of creep compliance derived from the data over a wide range of time and tem-

* To whom correspondence should be sent.

perature in the glassy state. In the case of dielectric β -relaxation too, measurement in comparable ranges of time and temperature should be made to derive the spectrum separated enough from the α -relaxation.

The present paper is concerned with determining the relaxation spectra for the dielectric β -processes in a series of poly(*n*-alkyl methacrylate)s from the data on absorption current. The major aim is to get more information on the motion of the side chain under the condition that the micro-Brownian motion of the main chain is completely frozen. The absorption current corresponds to the creep rate in the case of mechanical retardation. Consequently, the ranges of time and temperature for the measurement of absorption current can be taken as similar to those for the creep measurement. Another aim of the present study is to examine the validity and limitations of the method of reduced variables²⁰ when applied to loss permittivity obtained from the absorption current in the glassy state of this kind of polymers.

EXPERIMENTAL

Poly(methyl methacrylate) (PMMA), poly(ethyl methacrylate) (PEMA), poly(*n*-propyl methacrylate) (P*n*PMA), and poly(*n*-butyl methacrylate) (P*n*BMA) were used in this study. All these samples were atactic polymers prepared by bulk polymerization of purified monomers with or without benzoyl peroxide as an initiator. The polymers obtained were dissolved in benzene and cast into films. Each film was dried for several hours in vacuum at a temperature above the glass transition temperature to eliminate solvent and unreacted monomers. The thickness of the films ranged from 0.2 to 0.5 mm. A commercial sample of PMMA compression-molded into a sheet about 3 mm thick was also used for comparison. The degree of polymerization of each sample was not determined. All samples were dried again for several days in vacuum prior to each measurement in order to eliminate adsorbed water.

The absorption current was measured with the aid of a vibrating-reed electrometer, type TR-84M, made by Takeda Riken Industry Co. Dry cells were used as a d.c. voltage source and a three-electrode arrangement made by Ando Electric Co. was adopted. The effective area of the main electrode

was *ca.* 4.89 cm². The charging current was measured from 10 to 600 s after the application of a voltage at *ca.* 5°C intervals of temperature ranging from -90 to 20°C. The measurement was carried out from lower to higher temperatures. Temperature was determined by a copper-constantan thermocouple placed near the sample and its fluctuations during the measurement were kept within $\pm 0.5^\circ\text{C}$.

Preliminary experiments on the charging current carried out for three days at low temperatures showed that any leakage current should be very small. Therefore, the charging current was regarded substantially as the absorption current. After measuring the charging current at each temperature, the specimen was short-circuited while the temperature was raised for the next measurement. This procedure saved the time necessary to reduce the discharging current to the level of an experimental error.

In order to measure the absorption current under the condition that the linearity relation between current and voltage was assured, voltage dependence of the charging current was investigated at various temperatures and times elapsed. The field intensity in the samples ranged from *ca.* 100 to 6000 V cm⁻¹. All the data on the absorption current reported in the present paper satisfy the linearity condition.

In addition temperature dependences of loss and storage permittivities for PMMA and PEMA were measured at 0.1, 1, and 10 Hz in the temperature range from *ca.* -100 to 100°C with the ultra-low-frequency bridge apparatus, type TR-4, made by Ando Electric Co. Temperature of the sample was measured and kept constant in the same manner as in the case of the measurement of the absorption current.

RESULTS AND DISCUSSION

Calculation of Loss Permittivity from Absorption Current

Typical experimental results for the time dependence of the absorption current in PMMA and PEMA are illustrated in Figures 1 and 2. For each polymer only the data at temperatures in steps of *ca.* 10 or 15° are shown for the sake of clarity of the diagrams. For P*n*PMA and P*n*BMA similar results (not shown here) were obtained. The time de-

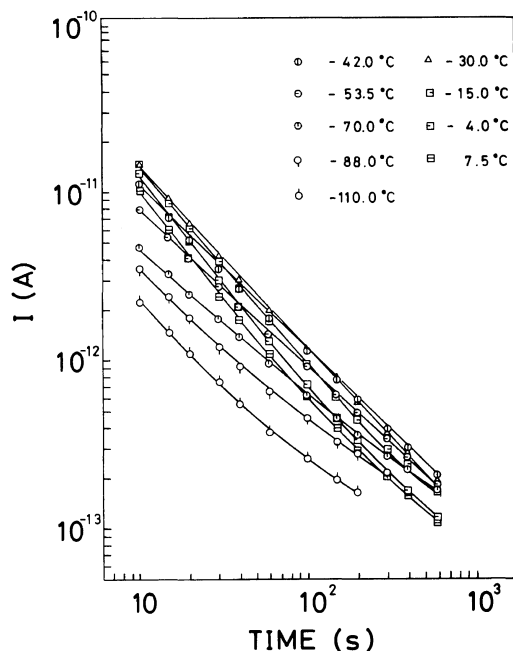


Figure 1. Time dependence of absorption current in poly(methyl methacrylate) at the temperatures indicated.

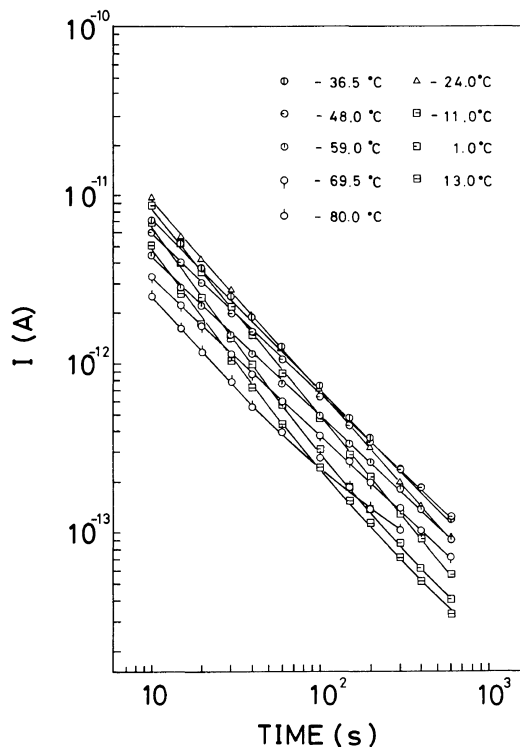


Figure 2. Time dependence of absorption current in poly(ethyl methacrylate) at the temperatures indicated.

pendence of the absorption current $I(t)$ as shown in these figures can be expressed approximately by a power function of time, $I(t) = At^{-n}$, where A and n are temperature dependent and n is close to unity. Actually, it was found that the range of numerical values of n was $0.84 \leq n \leq 1.30$ for PMMA, $0.66 \leq n \leq 1.25$ for PEMA, $0.77 \leq n \leq 1.22$ for PnPMA, and $0.74 \leq n \leq 1.06$ for PnBMA.

It is well-known that the frequency dependence of loss permittivity of a dielectric medium can be calculated from the data on the absorption current if the Hamon approximation is applicable.²¹ The formulas for this calculation are

$$\varepsilon''(\omega) = I(t)/\omega C_0 V \quad (1)$$

$$\omega t = 0.63 \quad (2)$$

where $\varepsilon''(\omega)$ is the loss permittivity at an angular frequency ω , C_0 is the capacitance of electrodes without the medium and V is the applied step voltage. According to Hamon, eq 1 and 2 can be used with good accuracy for the absorption current represented by the power function of time subject to the bounds

$$0.3 < n < 1.2 \quad (3)$$

Recently, several authors have investigated the use of the Hamon approximation for the absorption current with values of n outside those given by eq 3.²²⁻²⁵ The results of these investigations show that eq 1 and 2 are applicable over the entire range of time with a fairly good accuracy for the absorption current in a dielectric medium characterized by the Cole-Cole distribution of relaxation times with the Cole-Cole parameter $\beta < 0.3$.

Most of our data on the absorption current satisfy eq 3 and only some of the data have n -values slightly higher than the upper bound. On the other hand, the values of complex permittivity measured at low frequencies in the glassy state could be fitted to the Cole-Cole arc with the parameter $\beta < 0.3$. Therefore, we assume that eq 1 and 2 are applicable for all data on the absorption current in the four samples.

Loss Permittivity and Application of the Method of Reduced Variables

The loss permittivity curves at various temperatures obtained for the four samples by eq 1 and 2 are shown in Figures 3—6 as a function of the loga-

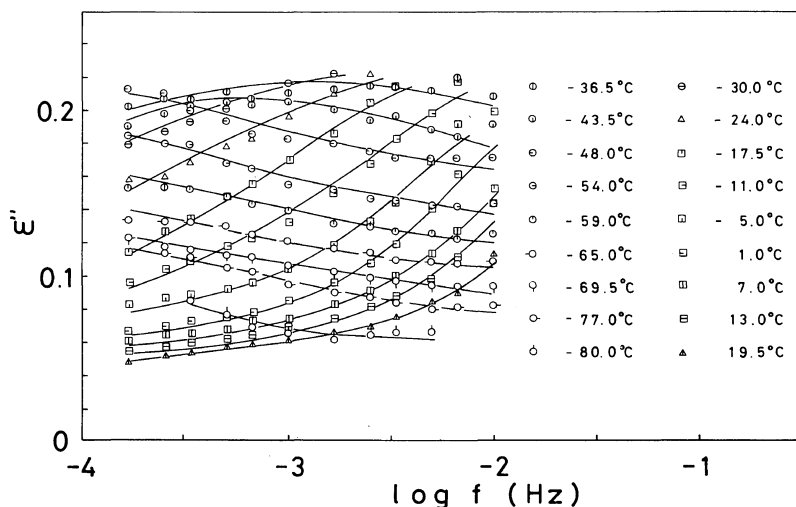


Figure 3. Frequency dependence of loss permittivity of poly(methyl methacrylate) calculated from absorption current at the temperatures indicated.

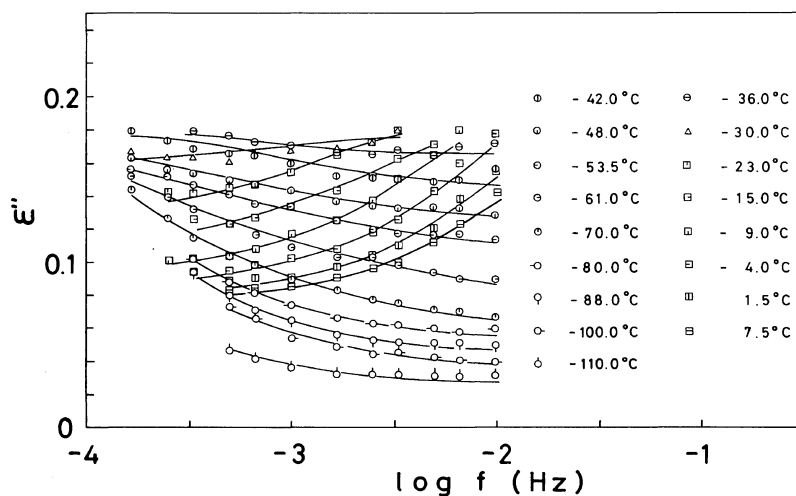


Figure 4. Frequency dependence of loss permittivity of poly(ethyl methacrylate) calculated from absorption current at the temperatures indicated.

rithm of frequency. From each of these figures the temperature dependence of loss permittivity at a fixed frequency can be determined. The loss permittivity vs. temperature curve thus obtained has a peak at a temperature which varies with the frequency fixed. In Figure 7, the frequency-temperature relations for such peaks for the four samples are illustrated. It is remarkable that these plots give parallel straight lines with an activation energy of *ca.* 19 kcal mol⁻¹ and that the straight line

for the sample with a longer side chain appears at higher temperatures.

In Figures 8 and 9, the loss peaks for PMMA and PEMA shown in Figure 7 are replotted along with those obtained by low-frequency measurements on the same samples and those by audio-frequency measurements reported by Ishida and Yamafuji.⁹ The results from the present data on the absorption current are in good agreement with those from the other higher frequency data. It should be noted also

Relaxation Spectroscopy of Poly(*n*-alkyl methacrylate)s

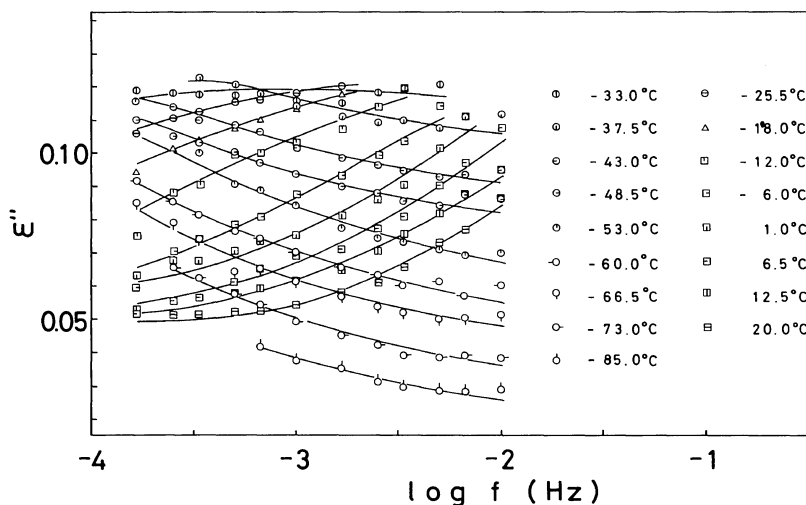


Figure 5. Frequency dependence of loss permittivity of poly(*n*-propyl methacrylate) calculated from absorption current at the temperatures indicated.

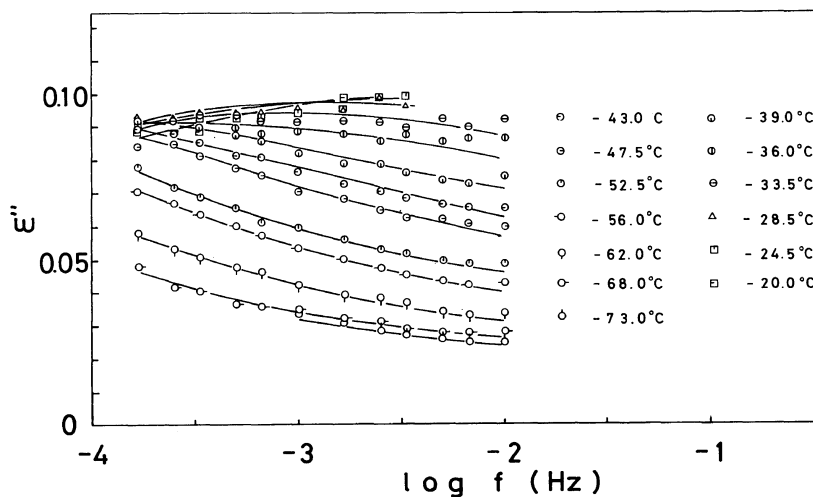


Figure 6. Frequency dependence of loss permittivity of poly(*n*-butyl methacrylate) calculated from absorption current at the temperatures indicated.

that the loss peaks in the audio-frequency region are taken from the data on the frequency dependence of loss permittivity, while those in the lower-frequency region are taken from the data on the temperature dependence of loss permittivity. Therefore, the agreement between these data indicates that the temperature dependence of the intensity of relaxation (relaxation strength) is rather weak.

In Figures 10—13, the master curves of ϵ'' for the four samples are shown; these have been obtained

from the data in Figures 3—6 by the method of reduced variables. Some data which feather off appreciably from the master curve were omitted. In the reduction procedure, only the shift along the $\log f$ axis was carried out. The shift factors for the four samples are shown in Figure 14, where the same reference temperature is chosen for the sake of comparison. All the shift factors are in good agreement with each other, and the activation energy determined from the slope of the solid straight line

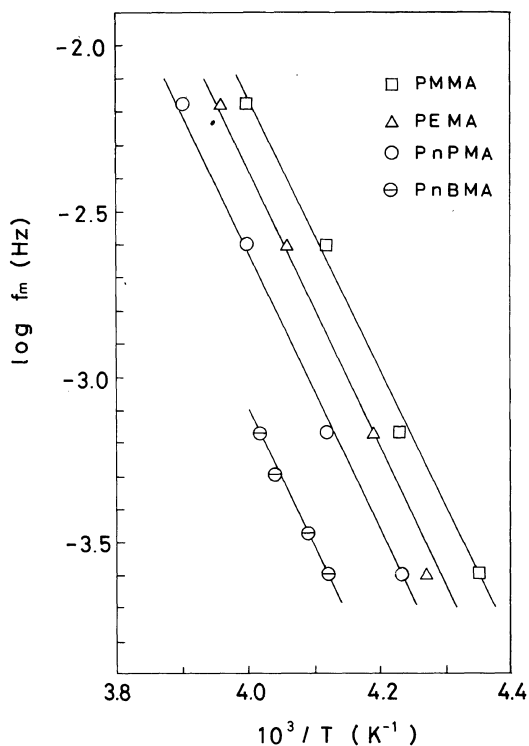


Figure 7. Plots of \log (frequency) against reciprocal of absolute temperature for the loss-permittivity maxima of PMMA, PEMA, PnPMA, and PnBMA appearing in temperature dependence of loss permittivity obtained from absorption current.

in Figure 14 is *ca.* 19 kcal mol^{-1} , which agrees very well with that obtained from Figures 7, 8, and 9. This fact supports the validity of the reduction procedure involving no correction for the temperature dependence of the limiting values of storage permittivity.

Shape of Loss Permittivity as a Function of Frequency

It is very interesting to compare the shape of the master curve of ϵ'' obtained from the data on the absorption current with that of the loss-permittivity curve obtained in the audio-frequency range. In Figure 15, the master curve of ϵ'' for PMMA is shown at four temperatures at which loss permittivity was measured in the audio-frequency range by Ishida and Yamafuji.⁹ The frequency-temperature position of the master curve is determined by the shift factor in Figure 14. It is

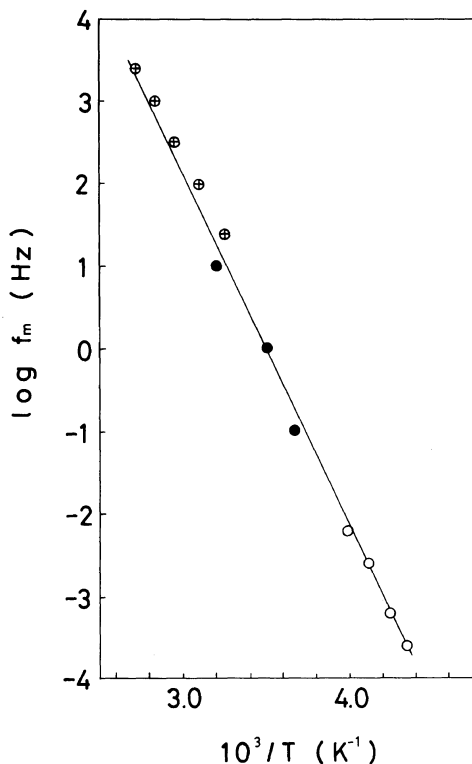


Figure 8. Plot of \log (frequency) against reciprocal of absolute temperature for the loss permittivity maxima of PMMA determined by absorption-current (open circles, T), ultra-low frequency (filled circles, T) and audio-frequency (crossed circles, f) measurements. Here T and f denote respectively temperature and frequency of maximum loss for constant-frequency and constant-temperature curves.

remarkable that the master curves at -66.0 , -26.3 , and -5.7°C can be connected very smoothly with the corresponding loss permittivity curves measured in the range of higher frequency. However, the shape of the loss permittivity curve becomes sharper at higher temperatures, so that the method of reduced variables cannot be used there. The critical temperature above which the sharpening of the loss permittivity curve sets in is estimated from Figure 15 to be about 9.7°C .

The very similar situation observed with PEMA is illustrated in Figure 16. In this case, the shift factor was determined below 7.5°C but the peak position of the master curve followed the straight line given in Figure 9. The agreement between the master curve thus shifted to 17.7°C and the loss

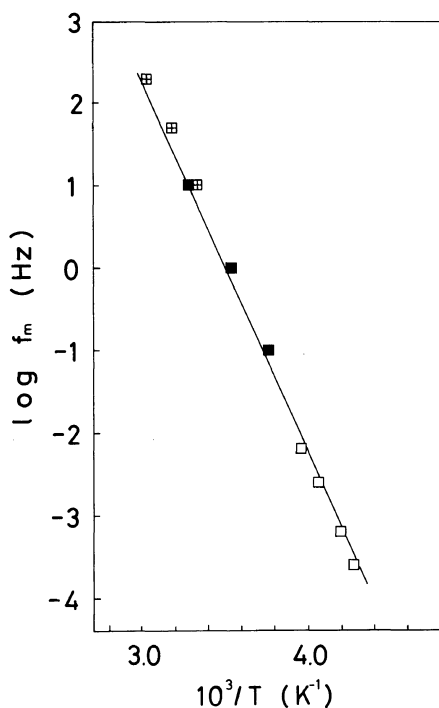


Figure 9. Plot of \log (frequency) against reciprocal of absolute temperature for the loss permittivity maxima of PEMA determined by absorption-current (open squares, T), ultra-low frequency (filled squares, T) and audio-frequency (crossed squares, f) measurements. Here T and f denote respectively temperature and frequency of maximum loss for constant-frequency and constant-temperature curves.

permittivity curve measured at this temperature by Ishida and Yamafuji⁹ is excellent. On the other hand, the shape of the loss permittivity curve becomes sharper with the increase in temperature above 17.7°C. Consequently, the critical temperature above which the sharpening of the curve for PEMA sets in lies between 17.7 and 28.3°C. As for PnPMA and PnBMA, the loss permittivity peak for the β -relaxation cannot be separated clearly from that for the α -relaxation in the audio-frequency range. Therefore, an analysis similar to those for PMMA and PEMA cannot be made.

In Figures 17 and 18, half-widths of the loss permittivity curves for PMMA and PEMA are plotted against temperature. In each of these figures the half-width changes with temperature in two steps, being constant at low temperatures, decreasing with the increase in temperature from the critical temperature up to the glass transition temperature T_g , then leveling off, and again decreasing at still higher temperatures. Although the molecular processes responsible for such a characteristic change of the spectral shape with temperature are not yet clear, it is noteworthy that the critical temperature for PMMA reminds us of the characteristic temperature found by Fischer *et al.* through the X-ray study of thermal fluctuations in polymer density.²⁶ Probably a motion of the main chain which grows up to the micro-Brownian motion above T_g sets in at this temperature. Such a motion of the main chain

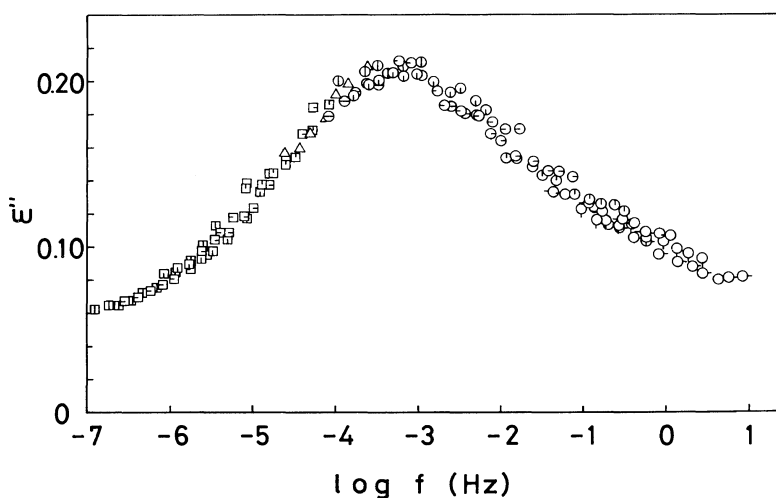


Figure 10. Master curve of loss permittivity for the β -relaxation in PMMA reduced to -43.5°C obtained from the data on absorption current. Temperature key is the same as in Figure 3.

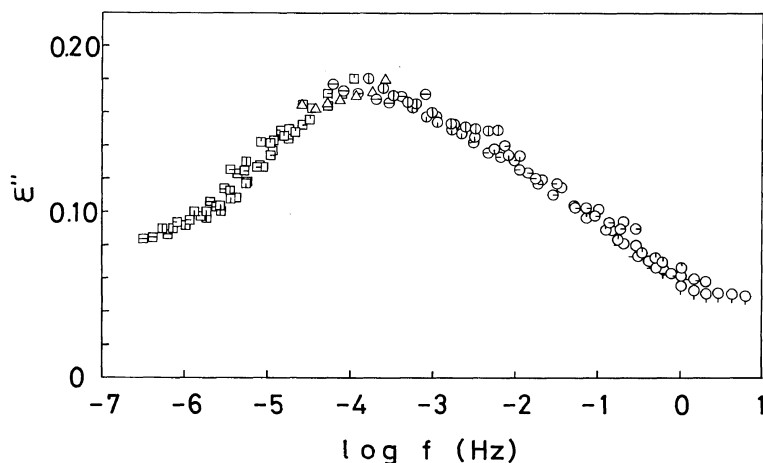


Figure 11. Master curve of loss permittivity for the β -relaxation in PEMA reduced to -42°C obtained from the data on absorption current. Temperature key is the same as in Figure 4.

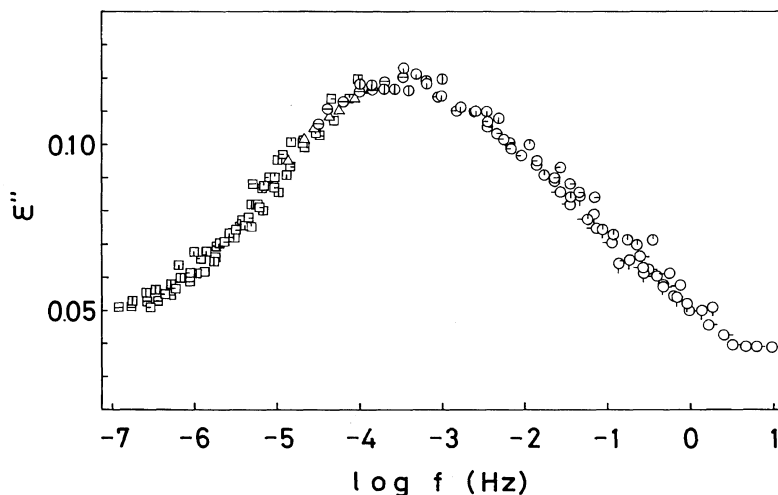


Figure 12. Master curve of loss permittivity for the β -relaxation in PnPMA reduced to -37.5°C obtained from the data on absorption current. Temperature key is the same as in Figure 5.

homogenizes the molecular environment of the side chains and thus should lead to the narrowing of the width of relaxation spectrum or loss permittivity curve.

Dielectric Relaxation Spectra for the β -Processes in the Four Samples

The dielectric relaxation spectrum in the zeroth approximation is given by

$$\phi(\ln \tau) = L_\epsilon(\ln \tau) / \Delta\epsilon = \frac{\pi}{2} \epsilon''(\omega) / \Delta\epsilon \Big|_{\omega=1/\tau} \quad (4)$$

where $\phi(\ln \tau)$ and $L_\epsilon(\ln \tau)$ are respectively normalized and non-normalized spectra as functions of the logarithm of the relaxation time τ and $\Delta\epsilon$ is the intensity of the dielectric relaxation. It should be noted that the dielectric relaxation corresponds to the mechanical retardation and so eq 4 corresponds to the approximation formula for the retardation spectrum.²⁰ The non-normalized β -spectra for the four samples are determined from the master curves of ϵ'' shown in Figures 10—13 and are illustrated in Figure 19.

It must be noted that the shape of the spectrum

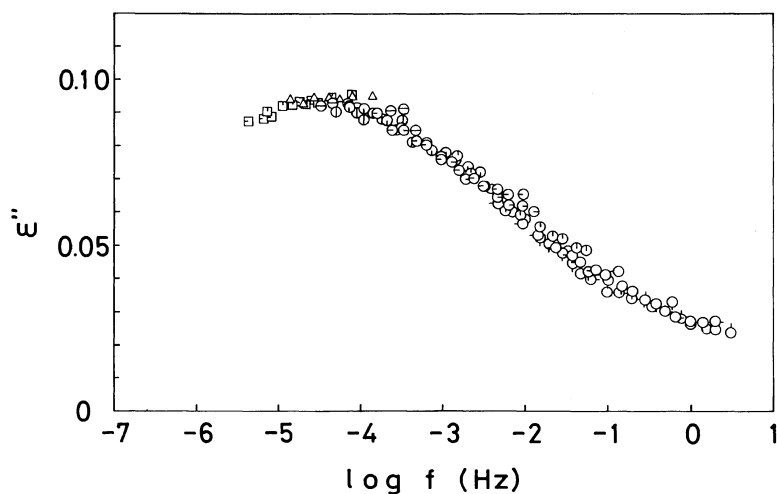


Figure 13. Master curve of loss permittivity for the β -relaxation in PnBMA reduced to -43.0°C obtained from the data on absorption current. Temperature key is the same as in Figure 6.

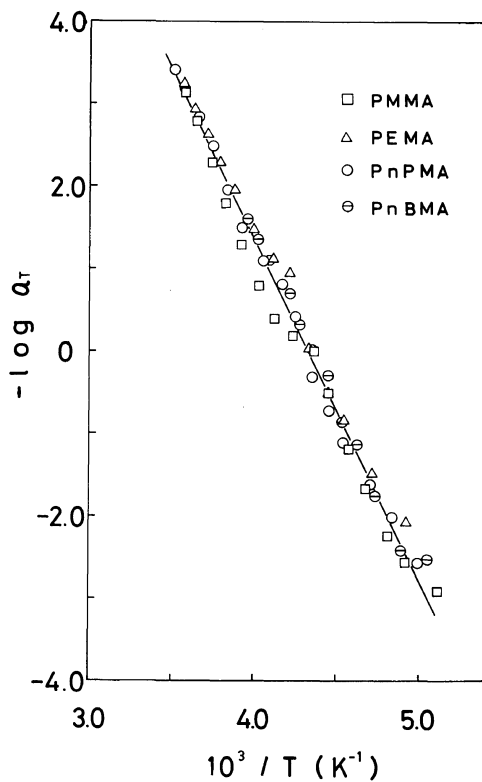


Figure 14. Plots of shift factors for the dielectric β -relaxations in PMMA, PEMA, PnPMA, and PnBMA reduced to -43.5°C against reciprocal of absolute temperature.

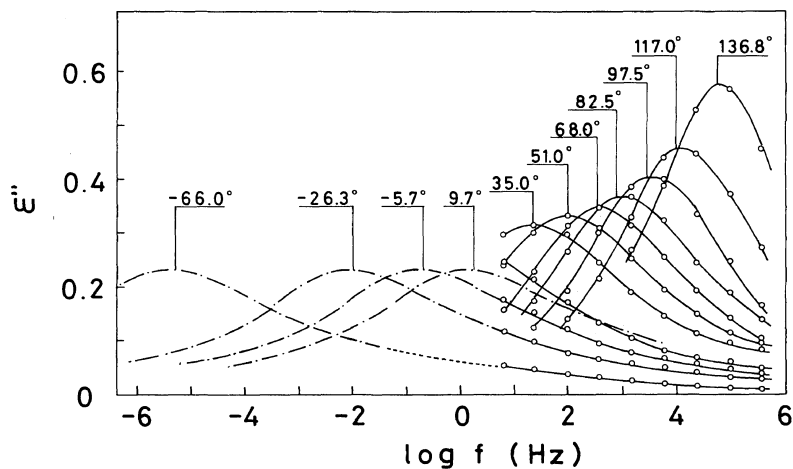


Figure 15. Frequency dependence of loss permittivity for the β -relaxation in PMMA at various temperatures obtained from absorption current (dashed dotted curves) compared with that determined by audio-frequency measurements by Ishida and Yamafuji⁹ (solid curves).

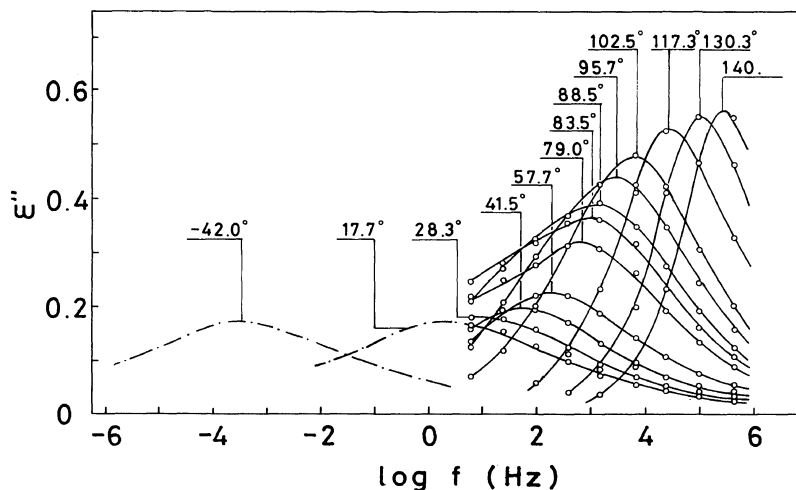


Figure 16. Frequency dependence of loss permittivity for the β -relaxation in PEMA at various temperatures obtained from absorption current (dashed dotted curves) compared with that determined by audio-frequency measurements by Ishida and Yamafuji⁹ (solid curves).

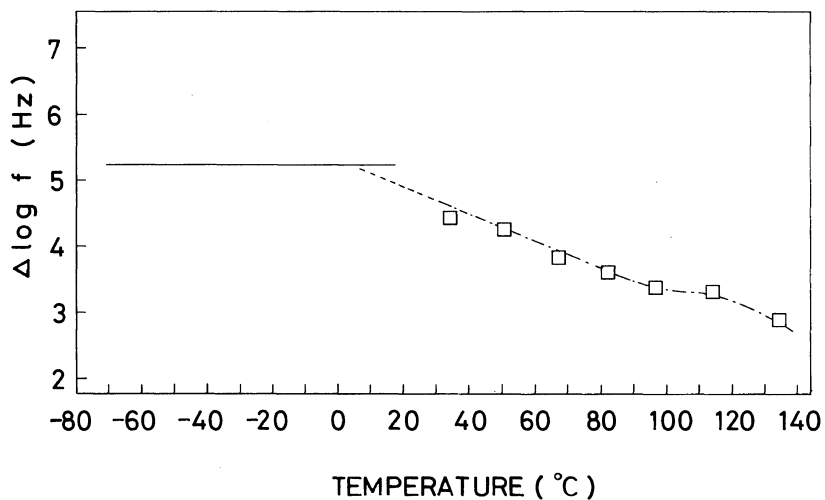


Figure 17. Temperature dependence of half-width of loss permittivity *versus* frequency plot for the β -relaxation in PMMA. Solid line represents the results obtained from the data on absorption current, while squares represent those on audio-frequency measurements by Ishida and Yamafuji.⁹

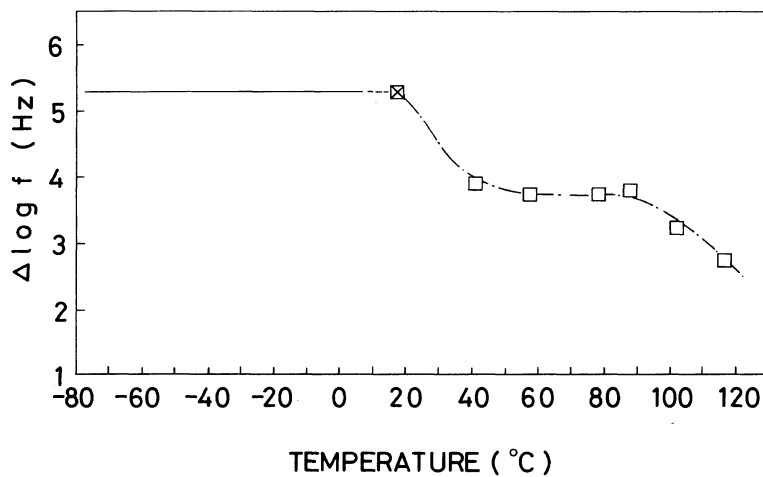


Figure 18. Temperature dependence of half-width of loss permittivity *versus* frequency plot for the β -relaxation in PEMA. Solid line represents the results obtained from the data on absorption current, while squares represent those on audio-frequency measurements by Ishida and Yamafuji.⁹ The crossed square denotes the point which is estimated by comparing the loss permittivity data in the audio-frequency range with those obtained from absorption current measurements.

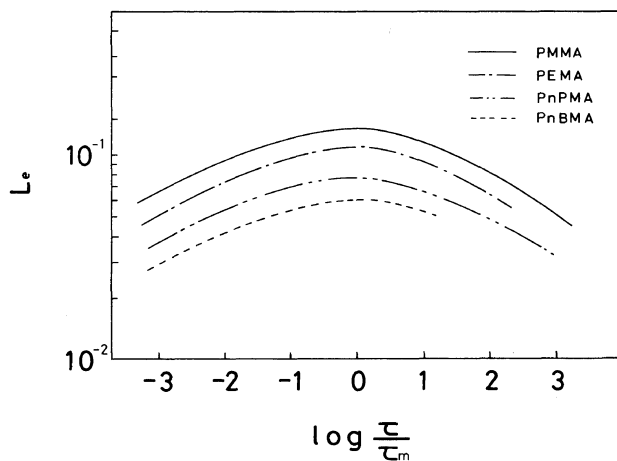


Figure 19. Dielectric β -relaxation spectra for PMMA, PEMA, PnPMA, and PnBMA plotted against logarithm of normalized relaxation time τ/τ_m , where τ_m denotes the relaxation time for the maximum of each spectrum. The peak heights are in the ratios 1:0.8:0.6:0.5.

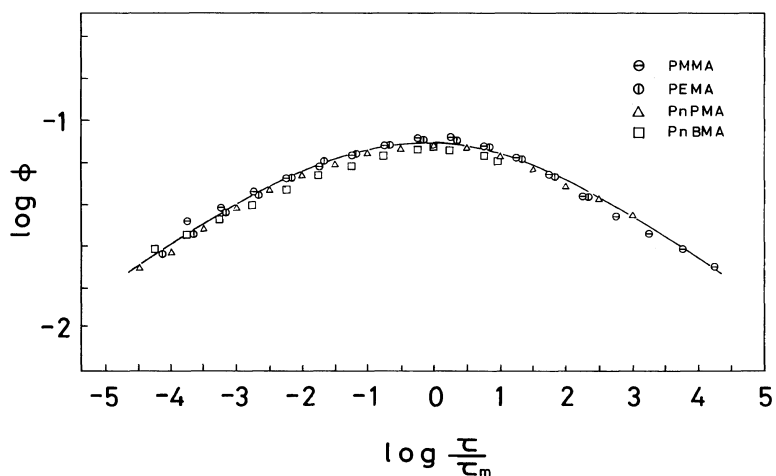


Figure 20. Dielectric β -relaxation spectra for PMMA, PEMA, PnPMA, and PnBMA normalized by their relaxation strength and plotted against logarithm of normalized relaxation time τ/τ_m , where τ_m denotes the relaxation time for the maximum of each spectrum.

Table I.

	Density ^a g cm ⁻³	N , Number of monomeric units per unit volume	N N for PMMA	$\Delta\epsilon$, dielectric relaxation strength	$\Delta\epsilon$ $\Delta\epsilon$ for PMMA	Ratio of reciprocal of side chain length to that for PMMA ^b
PMMA	1.18	7.1×10^{21}	1.0	1.6	1.0	1.0
PEMA	1.14	6.0×10^{21}	0.8	1.3	0.8	0.8
P <i>n</i> PMMA	1.09	5.1×10^{21}	0.7	1.0	0.6	0.6
P <i>n</i> BMA	1.07	4.5×10^{21}	0.6	0.8	0.5	0.5

^a Measured at -20°C (ref 27).

^b Side-chain length is the sum of bond lengths.

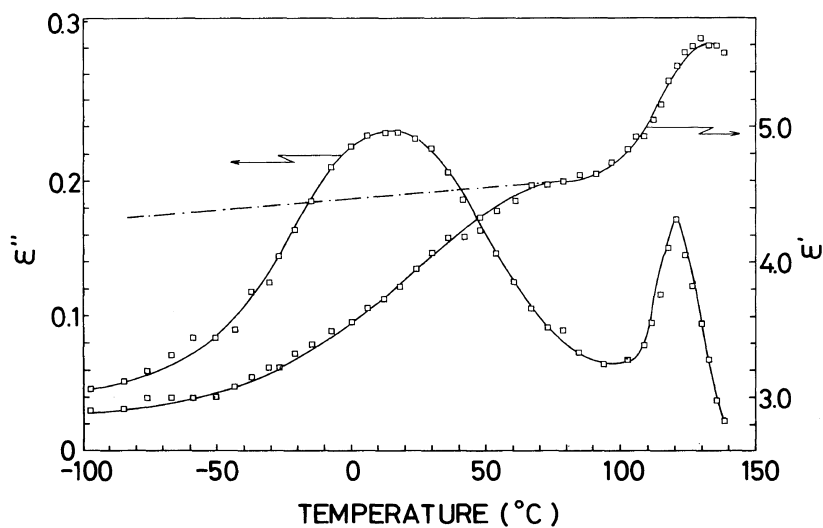


Figure 21. Temperature dependence of loss and storage permittivities for the α - and β -relaxations in PMMA at 1 Hz. The dashed dotted line drawn through the plateau region of storage permittivity represents temperature dependence of the low-frequency limit of storage permittivity for the β -relaxation.

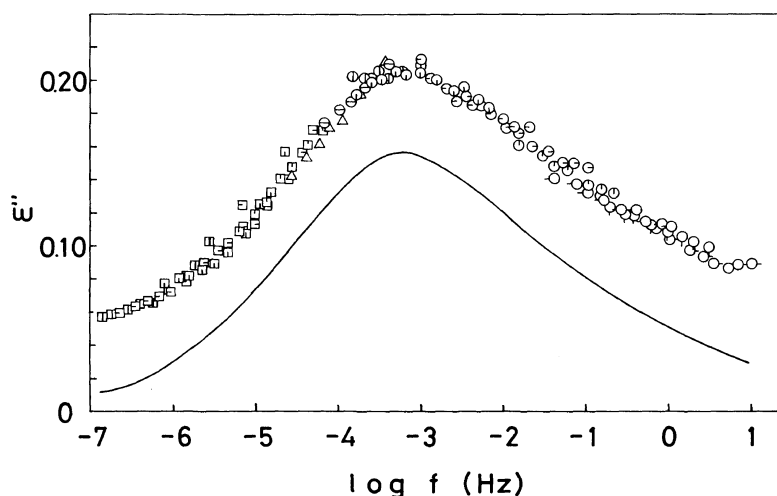


Figure 22. Master curve of loss permittivity for the β -relaxation in PMMA composed of the data corrected for temperature dependence of relaxation strength compared with that composed of the data not corrected (solid curve). Both curves are reduced to -43.5°C . Ordinate scale is correct for the corrected curve. The uncorrected curve has been shifted downward by 0.05.

thus obtained is independent of the side-chain length as shown in Figure 19. In other words, the logarithm of loss permittivity as a function of \log (frequency) has the shape which is independent of the side-chain length. Therefore, the intensity of the spectrum should be proportional to its peak height. The ratios of the peak heights of the dielectric-relaxation spectra for PMMA, PEMA, PnPMA, and PnBMA determined from Figure 19 are *ca.* 1 : 0.8 : 0.6 : 0.5.

On the other hand, the intensity of relaxation can be obtained from the area under the spectrum *versus* \log (retardation time) curve or that under the loss permittivity *versus* \log (frequency) curve by means of the relation,¹

$$\Delta\varepsilon = \int_{-\infty}^{\infty} L_e(\ln \tau) d \ln \tau = \frac{2}{\pi} \int_{-\infty}^{\infty} \varepsilon''(\omega) d \ln \omega \quad (5)$$

The area can be replaced approximately by that of the rectangle with the peak height and half-width of the spectrum or the loss permittivity curve as the two sides. The intensity of relaxation thus estimated is *ca.* 1.6 for PMMA, *ca.* 1.3 for PEMA, *ca.* 1.0 for PnPMA, and *ca.* 0.8 for PnBMA. The ratios between these values are also *ca.* 1 : 0.8 : 0.6 : 0.5. The spectra for the four samples normalized with these relaxation intensities are in excellent agreement with one another as shown in Figure 20.

Those ratios of relaxation intensities correspond to the ratios of the dipolar densities; *i.e.*, the numbers of monomeric units per unit volume of the four samples. Table I gives the sound basis for this interpretation. Here the values of density at temperatures lower than the critical temperatures mentioned above should be used. In this case, the values at -20°C ²⁷ are used somewhat arbitrarily, since the ratios are insensitive to the choice of the reference temperature. A similar result obtained from the data on the intensities of relaxation at the glass transition temperatures for these polymers was reported more qualitatively by Saito and Sasabe.¹⁹ In the present case, this relation holds at any temperature in the range where the method of reduced variables can be applied and suggests that each dipole in the side chain contributes to the β -relaxation nearly independently. It is interesting to note that the ratios mentioned above are quite similar to the ratios of the reciprocals of the side-chain lengths of the samples as shown in the last column of Table I.

Temperature Dependence of the Intensity of Relaxation

In the foregoing discussion, effect of the temperature dependence of the intensity of relaxation has been neglected. However, the intensity of relaxation

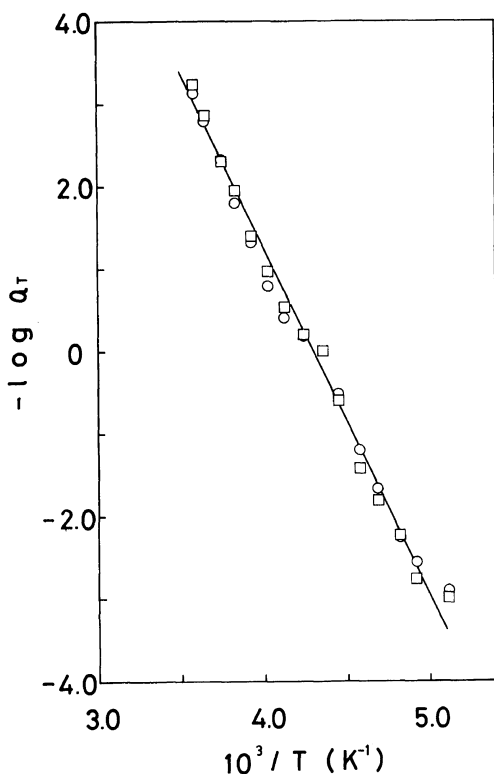


Figure 23. Plot of shift factor for the dielectric β -relaxation in PMMA reduced to -43.5°C against reciprocal of absolute temperature. Squares denote the values obtained from the data on loss permittivity corrected for temperature dependence of relaxation strength while circles denote those obtained from uncorrected data.

as a function of temperature should be investigated in order to get additional information on the nature of the β -relaxation, even though it has little effect on the relaxation spectrum and activation energy, as will be confirmed later.

In order to estimate the temperature coefficient of the intensity of relaxation, storage permittivity measured at 1 Hz has been used. In Figure 21, this quantity is plotted against temperature together with loss permittivity. The β -relaxation is separated rather clearly from the α -relaxation. The dashed dotted line having a slope of $1.2 \times 10^{-3} \text{ K}^{-1}$ through the stationary region at high temperatures is used to determine temperature variation of $\epsilon'(0)$, while the limiting value of ϵ' at low temperatures estimated to be *ca.* 2.9 is used for $\epsilon'(\infty)$ independent of temperature. The temperature coefficient of the

relaxation intensity and the values of $\epsilon'(0)$ and $\epsilon'(\infty)$ used here are in good agreement with those estimated from the data reported by Ishida and Yamafuji.⁹ Although the line representing the temperature dependence of the low-frequency limit of storage permittivity extends into the range where the shape of loss permittivity varies with temperature, the intensity of relaxation is assumed not to be affected by such a situation.

In Figure 22, the master curve of loss permittivity for PMMA corrected for the temperature dependence of the intensity of relaxation is compared with that without this correction. The two curves are almost the same; the uncorrected curve is represented here by a smoothed line and shifted downward by 0.05. The shift factors for these master curves are compared with each other in Figure 23. The agreement is excellent. Therefore, as has been assumed in the foregoing discussion, the effects of the temperature dependence of the relaxation intensity on the relaxation spectrum and activation energy are negligible. In addition, such a small temperature coefficient as determined from Figure 21 does not alter the ratios of the relaxation intensities discussed above.

Two-Site Model

The simplest molecular model for a dielectric relaxation process is the two-site model, which gives the intensity of relaxation associated with dipole reorientation between the two stable states by

$$\Delta\epsilon = \frac{4\pi N(\Delta\mu)^2}{3kT} \left(\frac{\epsilon_\infty + 2}{3} \right)^2 \left(\frac{3\epsilon_0}{2\epsilon_0 + \epsilon_\infty} \right) \frac{K}{(1+K)^2} \quad (6)$$

where N is the number of dipoles per unit volume, $\Delta\mu$ is the difference between the dipole moments at the two states, $K \equiv \exp(-\Delta G/kT)$ is an equilibrium constant with ΔG being the free energy difference between the two states, and ϵ_0 and ϵ_∞ are the low- and high-frequency limits of storage permittivity.²⁸

If K is much smaller than unity, the logarithm of $T\Delta\epsilon$ plotted against reciprocal absolute temperature should give a straight line. Figure 24 checks this prediction for PMMA. The values of relaxation intensity used in Figure 24 are the same as those used to compose the corrected master curve in Figure 22. The value of ΔG is determined from the slope of the straight line to be *ca.* 0.7 kcal mol⁻¹, which is similar to 0.9 kcal mol⁻¹ for *Pn*BMA reported by Sasabe.²⁹ If this value of ΔG is sub-

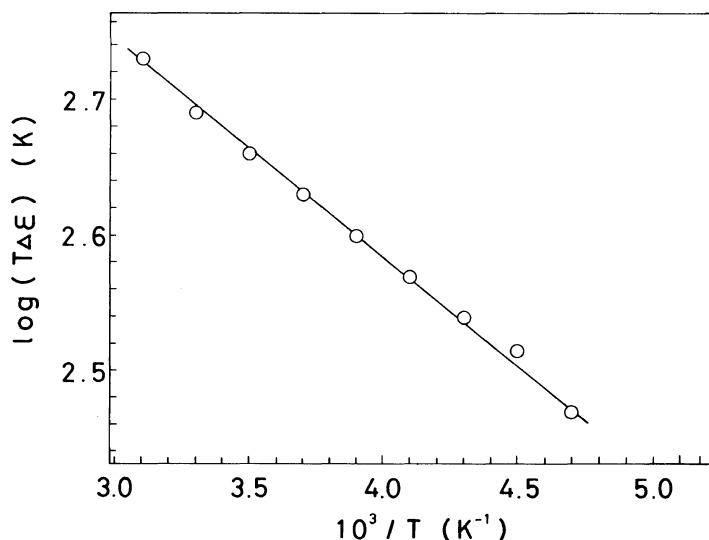


Figure 24. Plot of $\log(T\Delta\epsilon)$ for the β -relaxation in PMMA against reciprocal of absolute temperature. Temperature dependence of the relaxation strength $\Delta\epsilon$ is determined from the data on temperature dependence of storage permittivity at 1 Hz.

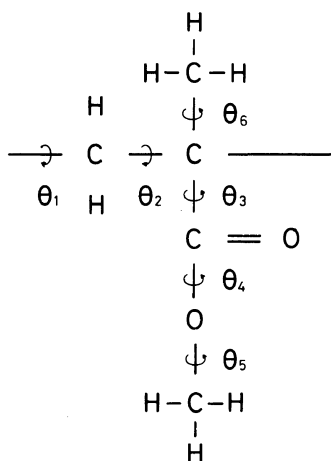


Figure 25. Internal-rotation angles for a monomeric unit of PMMA.

stituted along with the values of N , ϵ_0 , and ϵ_∞ at -20°C ($7.1 \times 10^{21} \text{ cm}^{-3}$, 4.4, and 2.9, respectively), $\Delta\mu$ is calculated from eq 6 to be 1.9 Debye. Here the value of N given in Table I is used for the number of dipoles per unit volume.

Therefore, if the PMMA molecule in the glassy state can take up two dipole orientation states which are associated with $\Delta\mu$ and ΔG similar to these values and separated by a barrier with the

activation energy of *ca.* 19 kcal mol $^{-1}$, the two-site model is useful for a semi-quantitative representation of the mechanism for the dielectric β -relaxation in PMMA and other methacrylate polymers in the glassy states. Tanaka and Ishida³⁰ determined energy contours for syndiotactic PMMA in a helicoidal conformation as a function of internal-rotation angles θ_3 and θ_4 shown in Figure 25, under the condition that θ_1 and θ_2 vary at intervals of 5° in the range of $\pm 15^\circ$ near the conformation of these angles as $(180^\circ, 180^\circ, -40^\circ, -40^\circ)$. According to their contour map, $(\theta_3 \doteq 45^\circ, \theta_4 \doteq 180^\circ)$ and $(\theta_3 \doteq 225^\circ, \theta_4 \doteq 180^\circ)$ seem to be two sites suitable for our case. Though our sample is atactic and not crystalline, we regard these two sites as those used in the foregoing discussion. The value of $\Delta\mu$ calculated geometrically for these two sites is *ca.* 2.8 Debye,¹⁹ which is in fair agreement with that calculated from eq 6.

The dielectric β -relaxation characterized by the spectrum of Figure 20 does not allow an accurate interpretation by the simple two-site model. However, the result obtained suggests that the motion of the side chain responsible for the β -relaxation extends over a scale as large as that for the transition between the above-mentioned two sites. Probably this motion of the side chain for the β -

process is associated with the local-mode motion of the main chain in the vicinity of its frozen conformation in the glassy state. The fact that the activation energy and the shape of the relaxation spectrum are almost independent of the side-chain length suggests strongly that there exists a general molecular mechanism for the β -process in the glassy state of poly(*n*-alkyl methacrylate)s.

REFERENCES

1. N. G. McCrum, B. E. Read, and G. Williams, "Anelastic and Dielectric Effects in Polymeric Solids," John Wiley & Sons, Inc., London, 1967.
2. E. A. W. Hoff, D. W. Robinson, and A. H. Willbourn, *J. Polym. Sci.*, **18**, 161 (1955).
3. J. D. Ferry, W. C. Child, Jr., R. Zand, D. M. Stern, M. L. Williams, and R. F. Landel, *J. Colloid Sci.*, **12**, 53 (1957).
4. W. C. Child, Jr. and J. D. Ferry, *J. Colloid Sci.*, **12**, 327 (1957).
5. W. C. Child, Jr. and J. D. Ferry, *J. Colloid Sci.*, **12**, 389 (1957).
6. G. P. Mikhailov and T. I. Borisova, *Soviet Phys. Tech. Phys.*, **3**, 120 (1958).
7. L. Brouckere and G. Offergeld, *J. Polym. Sci.*, **30**, 105 (1958).
8. J. Heijboer, *Makromol. Chem.*, **35A**, 86 (1960).
9. Y. Ishida and K. Yamafuji, *Kolloid Z.*, **177**, 97 (1961).
10. T. Hideshima, *Rep. Prog. Polym. Phys. Jpn.*, **6**, 143 (1963).
11. N. Saito, K. Okano, S. Iwayanagi, and T. Hideshima, "Solid State Physics," Vol. 14, Seitz and Turnbull, Ed., Academic Press, New York, 1963.
12. T. Hideshima, *Rep. Prog. Polym. Phys. Jpn.*, **9**, 281 (1966).
13. K. H. Illers, *Ber. Bunsenges. Phys. Chem.*, **70**, 353 (1966).
14. K. Kawamura, S. Nagai, J. Hirose, and Y. Wada, *J. Polym. Sci.*, *A-2*, **7**, 1559 (1969).
15. H. Shindo, I. Murakami, and H. Yamamura, *J. Polym. Sci.*, *A-1*, **7**, 297 (1969).
16. G. P. Mikhailov, *J. Tech. Phys. (USSR)*, **26**, 1924 (1956).
17. J. Heijboer, *Kolloid Z.*, **148**, 36 (1965).
18. G. Williams, *Trans. Faraday Soc.*, **62**, 2091 (1966).
19. H. Sasabe and S. Saito, *J. Polym. Sci.*, *A-2*, **6**, 1401 (1968).
20. J. D. Ferry, "Viscoelastic Properties of Polymers," 3rd ed, John Wiley & Sons, Inc., New York, 1980.
21. B. V. Hamon, *Proc. Inst. Electr. Eng.*, **99**, Part 4, 151 (1952).
22. T. Nakajima, *Bull. Electrotech. Lab. (Tokyo)*, **24**, 755 (1961).
23. G. Williams, *Trans. Faraday Soc.*, **58**, 1041 (1962).
24. M. E. Baird, *Rev. Mod. Phys.*, **40**, 219 (1968).
25. Y. Kita and N. Koizumi, *Adv. Mol. Relaxation Processes*, **7**, 13 (1975).
26. E. W. Fischer, J. H. Wendorff, M. Dettenmaier, G. Lieser, and I. Voigt-Martin, *J. Macromol. Sci., Phys.*, **B12**, 41 (1976).
27. S. S. Rogers and L. Mandelkern, *J. Phys. Chem.*, **61**, 985 (1957).
28. R. Hayakawa and Y. Wada, *J. Macromol. Sci., Phys.*, **B8**, 445 (1973).
29. H. Sasabe, *Res. Electrotech. Lab.*, **No. 721**, 50 (1971).
30. A. Tanaka and Y. Ishida, *J. Polym. Sci., Polym. Phys. Ed.*, **12**, 335 (1974).